

University of Portland Pilot Scholars

Physics Faculty Publications and Presentations

Physics

5-13-2009

Dynamical properties of an harmonic oscillator impacting a vibrating wall

O. F. de Alcantara Bonfim

University of Portland, bonfim@up.edu

Follow this and additional works at: http://pilotscholars.up.edu/phy_facpubs



Part of the [Quantum Physics Commons](#)

Citation: Pilot Scholars Version (Modified MLA Style)

Bonfim, O. F. de Alcantara, "Dynamical properties of an harmonic oscillator impacting a vibrating wall" (2009). *Physics Faculty Publications and Presentations*. 44.

http://pilotscholars.up.edu/phy_facpubs/44

This Journal Article is brought to you for free and open access by the Physics at Pilot Scholars. It has been accepted for inclusion in Physics Faculty Publications and Presentations by an authorized administrator of Pilot Scholars. For more information, please contact library@up.edu.

Dynamical properties of an harmonic oscillator impacting a vibrating wall

O. F. de Alcantara Bonfim*

Department of Physics, University of Portland, Portland, Oregon 97203, USA

(Received 11 February 2009; published 13 May 2009)

The dynamics of a spring-mass system under repeated impact with a vibrating wall is investigated using the static wall approximation. The evolution of the harmonic oscillator is described by two coupled difference equations. These equations are solved numerically, and in some cases exact analytical expressions have also been found. For a periodically vibrating wall, Fermi acceleration is only found at resonance. There, the average rebounding velocity increases linearly with the number of collisions. Near resonance, the average rebounding velocity grows initially with the number of collisions and eventually reaches a plateau. In the vicinity of resonance, the motion of the oscillator exhibits scaling properties over a range of frequency ratios. The presence of dissipation at resonance destroys the Fermi-acceleration process and induces scaling behavior similar to that at near resonance. For a moving wall with a random amplitude at collisions, Fermi acceleration is observed independently of the ratio between the wall and oscillator frequencies. In this case the average rebounding velocity grows with the square root of the number of collisions with the wall. Also, in this latter case, dissipation suppresses the Fermi-acceleration mechanism and induces a scaling behavior with the same universality class as that of the dissipative bouncing ball model with random external perturbations.

DOI: [10.1103/PhysRevE.79.056212](https://doi.org/10.1103/PhysRevE.79.056212)

PACS number(s): 05.45.Pq, 05.45.Tp, 05.45.Ac

I. INTRODUCTION

In an attempt to understand the origin of fast particles in cosmic rays, Fermi [1] proposed an acceleration mechanism to explain the high speed of these particles. Fermi's idea was that the cosmic ray particles would speed up as a result of the collisions between them and randomly moving magnetic fields existing in stellar space.

A mechanical analog of this mechanism was proposed by Ulam [2]. He suggested considering a system consisting of a light particle (or ball) moving between two horizontal very heavy walls, with one of them oscillating periodically. This model is known as the Fermi-Ulam model. One would expect that after many collisions the heavy wall would share its energy with the ball which, being lighter, would progressively accelerate indefinitely. Contrary to his and others' [3] expectations, numerical simulations of the model revealed that the average velocity of the particle did not become very large even after several thousand successive collisions, and no acceleration was found. The numerical simulations reported by Ulam [2] indicated that the motion of the ball appeared to be stochastic, but its energy on average did not increase with time. However, if the phase of the wall oscillation is chosen randomly at the time of the impact, then the particle is indeed accelerated on average.

Later Lichtenberg *et al.* [4,5] showed that the phase space structure for the model with a periodically oscillating wall was different, depending on the velocity of the particle. For instance, at low velocities the phase space is mostly chaotic; at intermediate velocity regions (islands) of regular motion are found imbedded in a chaotic sea and for large velocities the motion is, in general, regular and shows a limited gain of energy.

The effects of dissipation have been analyzed on the full model [6–10], as well as on a simplified version of the model

[9,11–13]. In the simplified version of the model, all collisions with the moving wall are assumed to take place at the same position. However, the velocity of the wall at the moment of collision is the same as if the wall was moving. This approximation is sometimes called the static wall approximation. Both versions of the model have recently been investigated where the moving wall is also stochastically oscillating [14–16].

A similar version of this model, first introduced by Pustyl'nikov [17], is known as the bouncer model. It consists of a particle bouncing vertically on an oscillating table under the action of a constant gravitational field. It has been shown that in the case of a periodic oscillating table Fermi acceleration is observed [4,5,17], that is, unlimited gain of energy for the particle depending on the initial conditions and control parameters. The system also exhibits a variety of dynamical behavior such as periodic motion, period-doubling cascade, and fully developed chaotic motion, depending on the amplitude and frequency of the vibration of the table.

The influence of damping on this model has also been investigated [18–30]. Experimental realizations of the bouncer model have been studied by several authors [22,31–36]. The inelastic bouncing ball has been used as a simplified model to understand the dynamics of vibrated granular media [37]. The Fermi-acceleration mechanism has been found to be useful to study phenomena in other areas of physics such as astrophysics [38–40], atomic physics [41], optics [42,43], and plasma physics [44,45]. Combining the Fermi-Ulam model with the bouncer model, a hybrid model was formed consisting of the bouncer with an additional fixed barrier parallel to the oscillating table. The dynamic properties of this hybrid model have been analyzed under several conditions [46,47].

Motivated by the study of these systems and their surprising dynamical behavior, in this work I investigate the dynamics of an harmonic oscillator undergoing repeated impact with a periodically vibrating heavy wall. A simplified version of this model, where the wall is kept in a fixed position and

*bonfim@up.edu

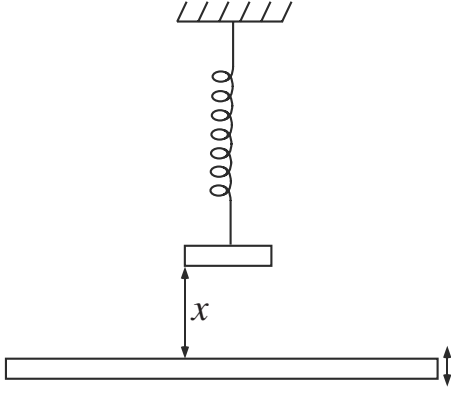


FIG. 1. Sketch of a spring-mass system which repeatedly collides with a vibrating wall.

the oscillator mass is subjected to a sinusoidal force, has been the subject of several studies both theoretically [48–55] and experimentally [55]. This system exhibits a multitude of complex behaviors such as period-doubling bifurcations leading to chaos [48–50,52], crises and hysteresis [52,54], grazing bifurcations [53,54], intermittent transition to chaos, and attractors showing the Devil’s stair-case behavior [52]. The case where both the oscillator and the wall are periodically vibrating has been used to model experiments involving an atomic force microscope [56,57].

This paper is arranged as follows. In Sec. II, the model is introduced in detail and the methods used to investigate it are outlined. In Sec. III, the results are presented and discussed.

II. MODEL

The system studied here consists of a mechanical oscillator, that is, a spring-mass system moving perpendicularly to a vibrating wall, as shown in Fig. 1. The rest position of the oscillator is placed at the equilibrium position of the wall. The natural frequency of the oscillator is ω_o , and in the case where the wall is held at its equilibrium position, all collisions with the wall will take place at time intervals $\Delta t = \pi/\omega_o$, corresponding to half of the oscillator period. It is assumed that the wall vibrates harmonically around the rest position of the oscillator with amplitude $x_w = x_o \sin(\omega t)$. Collisions will take place in the interval $[-x_o, x_o]$.

To simplify the analysis, the static wall approximation was used [4,5]. In this framework the wall is assumed to be fixed at the $x=0$ position at the moment of collision and exchanges momentum with the oscillator as if it was moving with velocity $\dot{x}_w = x_o \omega \cos(\omega t)$. This approximation has been applied to both the Fermi-Ulam [9,11–16] and bouncer [26–30] models. Under these conditions, the oscillator mass will repeatedly collide with the wall. Just after the n th collision, the oscillator mass will bounce off the wall with velocity u_n at time t_n . The next collision will take place at t_{n+1} , with the mass rebounding with velocity u_{n+1} . Since the time between collisions is $\Delta t = \pi/\omega_o$, this yields

$$t_{n+1} = t_n + \pi/\omega_o, \quad (1)$$

$$u_{n+1} = e u_n + (1 + e) \omega x_o \cos(\omega t_{n+1}), \quad (2)$$

where e is the coefficient of restitution between the oscillator mass and the vibrating wall. Defining the dimensionless variables $\phi_n = \omega t_n$, $v_n = u_n/\omega x_o$, and $r = \omega/\omega_o$, Eqs. (1) and (2) may be rewritten as

$$\phi_{n+1} = \phi_n + \pi r, \quad (3)$$

$$v_{n+1} = |e v_n + (1 + e) \cos(\phi_{n+1})|. \quad (4)$$

The absolute value has been added to the right-hand side of the velocity equation. This eliminates the nonphysical condition where the mass of the oscillator has a negative velocity after collision with the wall and would therefore move through the wall.

An important feature of the model used here springs from adopting the static wall approximation. Under this approximation all collisions take place at the equilibrium position of the oscillator. Hence the time between collisions is the same (half the period of the oscillator) and is independent of the velocity of the oscillator mass after collisions with the wall. As a consequence, the equations describing the evolution of the system are coupled in an asymmetrical fashion. Namely, the phase of the moving wall affects the velocity of the oscillator mass, but the latter does not change the phase. This makes it possible to obtain analytical solutions in various cases of interest.

In order to compare the present model with the results of the scaling behavior in the Fermi-Ulam and bouncer models, various quantities were introduced [58]. First, the cumulative velocity and cumulative square-velocity after n collisions are defined as

$$V_i^\gamma(r, e, n) = \frac{1}{n} \sum_{j=1}^n v_{i,j}^\gamma(r, e), \quad (5)$$

where $\gamma=1,2$. These quantities are calculated for a given initial condition for the phase and the rebounding velocity, labeled by the index i . By sampling over N initial conditions, the average of either quantity may be written as

$$\langle V^\gamma(r, e, n) \rangle = \frac{1}{n} \sum_{j=1}^n \langle v_j^\gamma(r, e) \rangle, \quad (6)$$

where $\langle V^\gamma(r, e, n) \rangle = \sum_{i=1}^N V_i^\gamma(r, e, n)/N$ and $\langle v_j^\gamma(r, e) \rangle = \sum_{i=1}^N v_{i,j}^\gamma(r, e)/N$. The cumulative velocity standard deviation is evaluated using

$$\Delta V(r, e, n) = \sqrt{\langle V^2(r, e, n) \rangle - \langle V(r, e, n) \rangle^2}. \quad (7)$$

The initial conditions for the phase are sampled from a random uniform distribution in the interval $[0, 2\pi)$. For simplicity, through out this work the initial condition $v_1=0$ is used for the rebounding velocity after the first collision. This sets the initial energy of the oscillator to zero. The above averages are calculated by sampling over $N=10^4$ initial conditions.

III. RESULTS AND CONCLUSIONS

The equation for the wall phase [Eq. (3)] can be readily integrated giving $\phi_n = \phi_1 + (n-1)\pi r$, where ϕ_1 is the phase of

the vibrating wall at the first collision. The velocity equation can also be found analytically as long as the expression inside the absolute value, namely, $f(v_n, \phi_{n+1}) = ev_n + (1 + e)\cos(\phi_{n+1})$, remains positive for all values of n , which can be found depending on a judicious choice of the initial conditions. Next the solutions to the velocity equation for various cases of interest are presented.

First consider the situation where the collisions are elastic ($e=1$) and analyze the dynamics of the system as a function of $r = \omega / \omega_o$. At resonance, that is for $r = 2k (k=1, 2, \dots)$ and if $\cos(\phi_1) \geq 0$, it is found that $f(v_n, \phi_{n+1}) \geq 0$ for all values of n . Thus, the velocity equation can be integrated to give $v_n = 2 \cos(\phi_1)(n-1)$. Therefore, the motion of the oscillator is unbounded and the rebounding velocity of the oscillator mass increases linearly with the number of collisions n (Fermi acceleration). If $\cos(\phi_1) < 0$, the absolute value in Eq. (4) cannot be discarded since the rebounding velocity may become negative immediately after a collision. Thus, no analytical solution can be found in this case. However, the values for $\langle v_n \rangle$ and $\langle v_n^2 \rangle$ can be exactly evaluated over the entire range of initial conditions for ϕ_1 , resulting in $\langle v_n \rangle = \frac{4}{\pi}(n-1)$ and $\langle v_n^2 \rangle = 2(n-1)^2$.

As pointed out earlier, the phase equation general solution is given by $\phi_{n+1} = \phi_1 + n\pi r$. Let $r = 2k \pm \xi$, where ξ measures the deviation from resonance. In the expression for the velocity [Eq. (4)], the phase enters as the argument of the cosine, yielding $\cos(\phi_{n+1}) = \cos(\phi_1 \pm n\pi\xi)$, which is independent of k . Therefore the behavior of the rebounding velocity near higher resonances is the same as for the first resonance. Because of that we only consider the motion of the oscillator near the first resonance ($k=1$), that is, $r = 2 \pm \xi$. For initial conditions with $\phi_1 < 3\pi/2$, the oscillator mass undergoes successive collisions until the phase of the wall reaches $\phi = 3\pi/2$ after $n^* = (3\pi/2 - \phi_1) / \pi\xi$ collisions. Beyond that point the rebounding velocity becomes non-negative and periodic. If $\phi_1 > 3\pi/2$, a transient is also observed until the phase of the wall reaches $\phi = 2\pi + 3\pi/2$ after $n^* = (2\pi + 3\pi/2 - \phi_1) / \pi\xi$ collisions, beyond which the rebounding velocity is also non-negative and periodic, as shown in Fig. 2. If $\phi_1 = 3\pi/2$, then $f(v_n, \phi_{n+1}) \geq 0$ for $n \geq 1$. Therefore, the velocity equation can be integrated yielding $v_n(\xi) = \frac{4}{\pi\xi} \sin^2[\pi\xi(n-1)/2]$, with $\xi \ll 1$. This expression indicates that the rebounding velocity of the mass is limited, grows at a rate inversely proportional to ξ , and varies sinusoidally with the number of collisions n . Although this result is valid only if $\phi_1 = 3\pi/2$, it shows a important point, namely, that the dependence on ξ may be scaled out using the reduced variables v_n / ξ^α and $(n-1) / \xi^z$, with $\alpha = z = -1$. A numerical fit for the average rebounding velocity over all ϕ_1 leads to $\langle v_n \rangle = \{A_1(1 - e^{-B_1[(n-1)\xi]^2})\}^{1/2} / \xi$, with $A_1 = 0.406(1)$ and $B_1 = 1.09(1)$. This indicates that the scaling behavior persists for all values of ϕ_1 even where no analytical solution is found. Similarly, for the average rebounding square velocity one gets $\langle v_n^2 \rangle = A_2(1 - e^{-B_2[(n-1)\xi]^2}) / \xi^2$, with $A_2 = 0.608(1)$ and $B_2 = 1.73(1)$. These fitted expressions are for all practical purposes indistinguishable from their corresponding values calculated directly from Eqs. (3) and (4). In Fig. 3, the behavior of the cumulative velocity standard deviation is plotted as a function of the number of collisions for several values of ξ ,

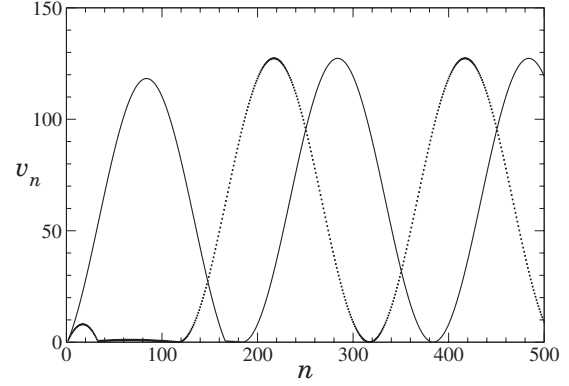


FIG. 2. Rebounding velocity of the oscillator mass as a function of the number of collisions n for $\xi = 10^{-2}$ in the elastic case, with initial conditions $(\phi_1, v_1) = (\pi/3, 0)$ (dotted line) and $(\phi_1, v_1) = (5\pi/3, 0)$ (solid line). In both cases a transient persists until the phase of the moving wall reaches $\phi = 3\pi/2$, beyond which the rebounding velocity becomes periodic.

from 10^{-2} to 10^{-6} . Observe that ΔV initially grows linearly with the number of collisions and rapidly changes to a saturated value ΔV_s beyond a crossover value n_x . By analyzing the plots following the procedure used in [58], one arrives at the following results:

$$\Delta V(\xi, n) \propto n^\beta \quad [n \ll n_x] \quad \text{with } \beta = +1.00(2), \quad (8)$$

$$\Delta V_s(\xi) \propto \xi^\alpha \quad [n \gg n_x] \quad \text{with } \alpha = -1.00(1), \quad (9)$$

$$n_x \propto \xi^z \quad \text{with } z = -1.00(1), \quad (10)$$

where the exponents α and z agree with the analytical values calculated above. Using the scaling concepts discussed in [58], it is found that the set of exponents (α, β, z) are not independent but related by $z = \alpha / \beta$. Also the standard deviation of the cumulative velocity obeys the scaling relation

$$\Delta V(\xi, n) \sim \xi^\alpha f(n/\xi^z), \quad (11)$$

where $f(u)$ is a universal scaling function which can be found for the data in Fig. 3 by plotting $\Delta V / \xi^\alpha$ versus n / ξ^z as

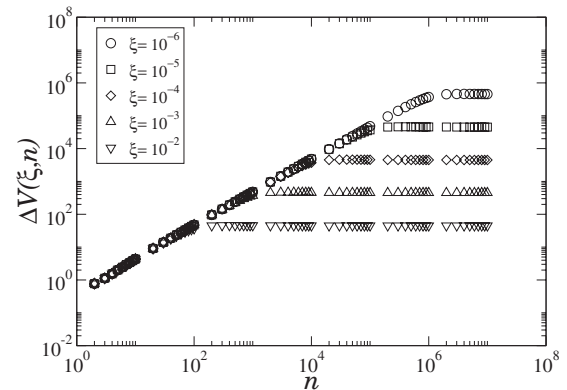


FIG. 3. Rebounding velocity standard deviation versus the number of collisions near resonance for several values of ξ . Here the collisions with the wall are elastic.

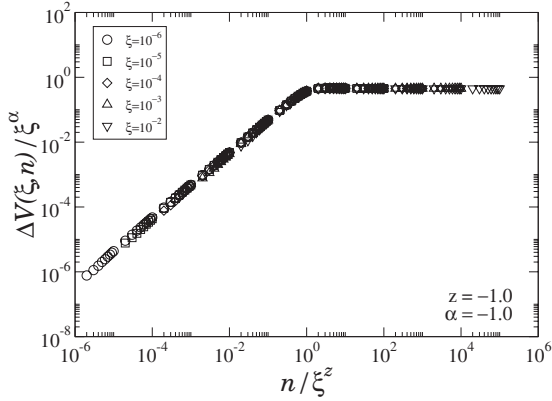


FIG. 4. Reduced cumulative velocity standard deviation in terms of scaled number of collisions near resonance. Using the scaling exponents $(\alpha, z) = (-1, -1)$, the curves collapse into a single curve for all ξ .

shown in Fig. 4, where all curves collapse into a single scaling function.

Now consider the case where the system is at resonance, that is, $\xi=0$, with inelastic collisions. First take the coefficient of restitution close to unity, $e=1-\zeta$, where $\zeta \ll 1$. In this case, one can also find a closed expression for the rebounding velocity by integrating Eq. (4), as long as $\cos(\phi_1) \geq 0$, namely, $v_n(\zeta) = \frac{2}{\zeta} \cos(\phi_1) [1 - e^{-\zeta(n-1)}]$.

This result shows that for a range of initial conditions, the effects of dissipation can also be scaled out by introducing the reduced variables v_n/ζ^α and $(n-1)/\zeta^z$, with $\alpha=z=-1$, as in the elastic case near resonance previously discussed. A numerical fit for $\langle v_n \rangle$ averaged over all ϕ_1 yields $\langle v_n \rangle = A_1 [1 - e^{-\zeta(n-1)}] / \zeta$, with $A_1 = 0.64(1)$, and similarly $\langle v_n^2 \rangle = \{A_2 [1 - e^{-\zeta(n-1)}] / \zeta\}^2$, with $A_2 = 1.00(1)$.

In Fig. 5 the cumulative velocity standard deviation is plotted against the number of collisions for several values of ζ . Initially ΔV grows with a power-law behavior for each ζ . Eventually it reaches a plateau similar to the behavior in the case of elastic collisions. As previously, there is a crossover at n_x between the two regimes, which is determined by the intersection of the two tangents to the power-law curves. Scaling is also observed in this case.

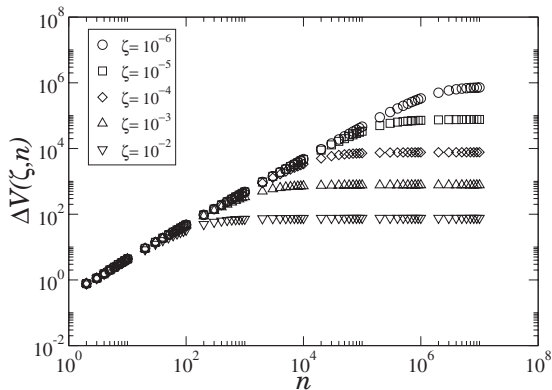


FIG. 5. Rebounding velocity standard deviation versus the number of collisions at resonance and in the presence of dissipation for several values of the coefficient of restitution $e=1-\zeta$.

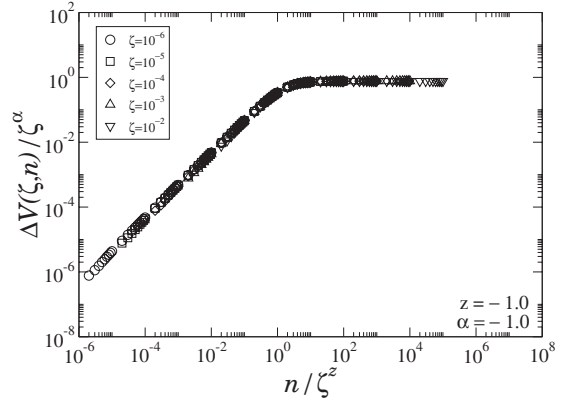


FIG. 6. Reduced cumulative velocity standard deviation in terms of scaled number of collisions at resonance and in the presence of dissipation. Using the scaling exponents $(\alpha, z) = (-1, -1)$, the curves collapse into a single curve for all ζ .

Figure 6 shows the collapse of the curves for different dampings into a single curve. It was found that the dynamical exponents z and α are the same as in the case of no damping, indicating that both cases belong to the same universality class. It must be pointed out that the scaling properties found in the present model do not involve chaos in the region of limited energy, unlike the Fermi-Ulam [9,11,12] and bouncer [26-28,30] models.

In the velocity equation [Eq. (4)], the change in velocity comes from two different mechanisms. The first is due to the nature of the inelastic collisions that reduces the rebounding velocity by a factor ev_n , with $e < 1$. The second corresponds to the transfer of momentum between the oscillator mass and the moving wall. This term is the one responsible for the Fermi acceleration.

To simplify our discussion, consider the extreme case where the transfer of momentum from the wall to the mass is at its maximum at every collision. Thus the velocity equation reads as $v_{n+1} = ev_n + (1+e)$. From this equation it is clear that the velocity change due to momentum transfer, $(1+e)$, is fixed and independent of the velocity of the oscillator mass. On the other hand, the reduction in velocity due to inelastic collisions depends on the velocity of the oscillator mass. For low velocities, the second term dominates and the velocity of the oscillator mass increases after each collision. However, as the velocity increases the first term will become more and more dominant until the contribution from each term cancels out the other leading to the limiting velocity $v_L = (1+e)/(1-e)$ and to the suppression of Fermi acceleration. The actual limiting velocity averaged over many initial conditions is in fact smaller than the value found above since the momentum transfer term is between $-(1+e)$ and $(1+e)$ for an arbitrary collision with the wall. A numerical expression for the average rebounding velocity as a function of the number of collisions is reported above.

By adding random perturbation to the phase of the vibrating wall, the finite difference equations for phase and velocity become

$$\phi_{n+1} = \phi_n + \pi r + R_{2\pi}(n), \tag{12}$$

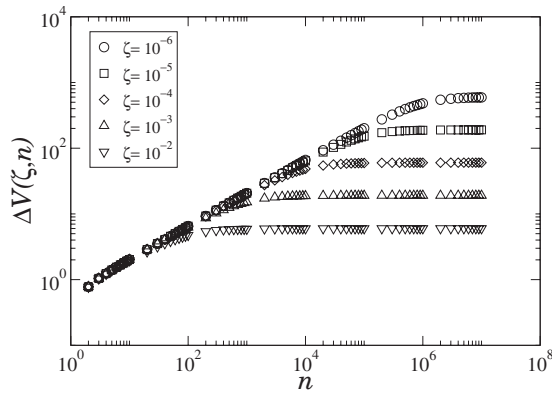


FIG. 7. Effects of dissipation on the standard deviation of the cumulative velocity in terms of number of collisions for several coefficients of restitution $e = 1 - \zeta$ when the wall phase at collision is random.

$$v_{n+1} = |ev_n + (1 + e)\cos(\phi_{n+1})|, \quad (13)$$

where $R_{2\pi}(n)$ is a uniform random number on the interval $[0, 2\pi)$.

For elastic collisions, the random perturbation modifies the functional dependence of the average rebounding velocity with the number of collisions. As discussed earlier, in the unperturbed elastic case, the rebounding velocity grows linearly with n . In the present case, however, the randomness induces a square-root dependence on n , which is found numerically to be $\langle v_n \rangle = [A_1(n-1)]^{1/2}$, with $A_1 = 1.273(2)$. However, the mean-square rebounding velocity can be calculated exactly by direct integration of Eq. 14, yielding $\langle v_n^2 \rangle = 2(n-1)$. It turns out that the ratio between the frequencies, r , becomes irrelevant when random perturbation is introduced due to the periodicity of the cosine.

When dissipation is present an exact expression for $\langle v_n^2 \rangle$ can also be found, obtained again by direct integration of Eq. 14, $\langle v_n^2(\zeta) \rangle = \frac{1}{\zeta} [1 - e^{-2\zeta(n-1)}]$. This expression shows that in the dissipative regime the mean-square rebounding velocity can be described by scalable variables. Numerical calculations clearly show that the same is observed for the average rebounding velocity, giving $\langle v_n \rangle = \{A_1 [1 - e^{-2\zeta(n-1)}] / \zeta\}^{1/2}$, with $A_1 = 0.636(1)$. The expressions for $\langle v_n \rangle$ and $\langle v_n^2 \rangle$ show that scaling is observed with critical exponents $(\alpha, z) = (-\frac{1}{2}, -1)$. These are the same exponents found in the dissipative bouncing model with random external perturbations [27], placing

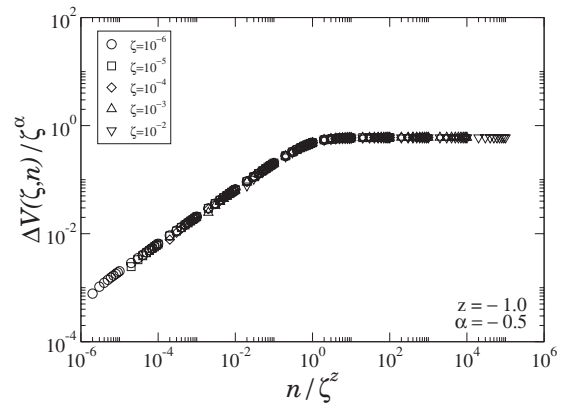


FIG. 8. Effects of dissipation on the reduced cumulative velocity standard deviation in terms of scaled number of collisions when the wall phase at collision is random. For $(\alpha, z) = (-\frac{1}{2}, -1)$, the curves collapse into a single curve for all values of ζ .

both models in the same universality class. The effects of dissipation on the cumulative velocity standard deviation as a function of the number of collisions with the wall are shown in Fig. 7 for several values of ζ of the coefficient of restitution.

These curves can also be made to collapse by using numerical fits to the power-law behaviors clearly identified in Fig. 7 for both the small and large numbers of collision regimes. The collapse is shown in Fig. 8 using the theoretical values for the exponents found above.

In summary, the behavior of an harmonic oscillator undergoing repeated impacts with a moving wall has been studied. For elastic collisions Fermi acceleration is observed at resonance when the wall is moving sinusoidally and for any frequency ratios when the phase of the moving wall at collisions is random. Near resonance Fermi acceleration is suppressed, and the rebounding velocity exhibits scaling properties. For inelastic collisions, the rebounding velocity is limited, exhibiting scaling at resonance when the motion of the wall is periodic and for any frequency ratios when the phase of the moving wall is selected randomly at collisions.

ACKNOWLEDGMENT

The author acknowledges support from the Murdock College Science Research Program.

- [1] E. Fermi, Phys. Rev. **75**, 1169 (1949).
 [2] S. Ulam, *Proceedings of the Fourth Berkeley Symposium on Mathematics, Statistics, and Probability Phenomena* (University of California Press, Berkeley, CA, 1961), Vol. 3, p. 315.
 [3] J. M. Hammersely, in Ref. [2], p. 79.
 [4] A. J. Lichtenberg, M. A. Lieberman, and R. H. Cohen, Physica D **1**, 291 (1980).
 [5] A. J. Lichtenberg and M. A. Lieberman, *Regular and Chaotic Dynamics*, Applied Mathematical Sciences Vol. 38 (Springer,

New York, 1992).

- [6] G. A. Luna-Acosta, Phys. Rev. A **42**, 7155 (1990).
 [7] K. Szymanski and Y. Labaye, Phys. Rev. E **59**, 2863 (1999).
 [8] E. D. Leonel and P. V. E. McClintock, J. Phys. A **38**, L425 (2005).
 [9] J. K. L. da Silva, D. G. Ladeira, E. D. Leonel, P. V. E. McClintock, and S. O. Kamphorst, Braz. J. Phys. **36**, 700 (2006).
 [10] E. D. Leonel, D. F. M. Oliveira, and R. E. de Carvalho, Physica A **386**, 73 (2007).

- [11] E. D. Leonel, P. V. E. McClintock, and J. K. L. da Silva, *Phys. Rev. Lett.* **93**, 014101 (2004).
- [12] D. G. Ladeira and Jafferson Kamphorst Leal da Silva, *Phys. Rev. E* **73**, 026201 (2006).
- [13] E. D. Leonel and P. V. E. McClintock, *Phys. Rev. E* **73**, 066223 (2006).
- [14] A. K. Karlis, P. K. Papachristou, F. K. Diakonou, V. Constantoudis, and P. Schmelcher, *Phys. Rev. Lett.* **97**, 194102 (2006).
- [15] A. K. Karlis, P. K. Papachristou, F. K. Diakonou, V. Constantoudis, and P. Schmelcher, *Phys. Rev. E* **76**, 016214 (2007).
- [16] A. K. Karlis, F. K. Diakonou, V. Constantoudis, and P. Schmelcher, *Phys. Rev. E* **78**, 046213 (2008).
- [17] L. D. Pustynnikov, *Trans. Mosc. Math. Soc.* **2**, 1 (1978).
- [18] C. N. Bapat, S. Sankar, and N. Popplewell, *J. Sound Vib.* **108**, 99 (1986).
- [19] A. Mehta and J. M. Luck, *Phys. Rev. Lett.* **65**, 393 (1990).
- [20] J. M. Luck and A. Mehta, *Phys. Rev. E* **48**, 3988 (1993).
- [21] A. C. J. Luo and R. P. S. Han, *Nonlinear Dyn.* **10**, 1 (1996).
- [22] C. R. de Oliveira and P. S. Goncalves, *Phys. Rev. E* **56**, 4868 (1997).
- [23] M. A. Naylor, P. Sánchez, and M. R. Swift, *Phys. Rev. E* **66**, 057201 (2002).
- [24] S. Giusepponi and F. Marchesoni, *Europhys. Lett.* **64**, 36 (2003).
- [25] S. N. Majumdar and M. J. Kearney, *Phys. Rev. E* **76**, 031130 (2007).
- [26] D. G. Ladeira and J. K. L. da Silva, *J. Phys. A* **40**, 11467 (2007).
- [27] E. D. Leonel, *J. Phys. A* **40**, F1077 (2007).
- [28] E. D. Leonel and A. L. P. Livorati, *Physica A* **387**, 1155 (2008).
- [29] E. D. Leonel and M. R. Silva, *J. Phys. A* **41**, 015104 (2008).
- [30] Andre Luis Prando Livorati, D. G. Ladeira, and E. D. Leonel, *Phys. Rev. E* **78**, 056205 (2008).
- [31] M. Franaszek and Z. J. Kowalik, *Phys. Rev. A* **33**, 3508 (1986).
- [32] P. Pierański and J. Małecki, *Phys. Rev. A* **34**, 582 (1986).
- [33] Z. J. Kowalik, M. Franaszek, and P. Pierański, *Phys. Rev. A* **37**, 4016 (1988).
- [34] K. Wiesenfeld and N. B. Tufillaro, *Physica D* **26**, 321 (1987).
- [35] S. Celaschi and R. L. Zimmerman, *Phys. Lett. A* **120**, 447 (1987).
- [36] C. Soria, A. Ramos, and A. T. Péres, *Europhys. Lett.* **37**, 541 (1997).
- [37] J. M. Hill, M. J. Jennings, D. V. To, and K. A. Williams, *Appl. Math. Model.* **24**, 715 (2000).
- [38] M. A. Malkov, *Phys. Rev. E* **58**, 4911 (1998).
- [39] K. Kobayakawa, Y. S. Honda, and T. Samura, *Phys. Rev. D* **66**, 083004 (2002).
- [40] A. Veltri and V. Carbone, *Phys. Rev. Lett.* **92**, 143901 (2004).
- [41] G. Lanzano *et al.*, *Phys. Rev. Lett.* **83**, 4518 (1999).
- [42] A. Steane, P. Szriftgiser, P. Desbiolles, and J. Dalibard, *Phys. Rev. Lett.* **74**, 4972 (1995).
- [43] F. Saif, I. Bialynicki-Birula, M. Fortunato, and W. P. Schleich, *Phys. Rev. A* **58**, 4779 (1998).
- [44] G. Michalek, M. Ostrowski, and R. Schlickeiser, *Sol. Phys.* **184**, 339 (1999).
- [45] A. V. Milovanov and L. M. Zelenyi, *Phys. Rev. E* **64**, 052101 (2001).
- [46] E. D. Leonel and P. V. E. McClintock, *J. Phys. A* **38**, 823 (2005).
- [47] T. W. Burkhardt and S. N. Kotsev, *Phys. Rev. E* **73**, 046121 (2006).
- [48] J. M. T. Thompson and R. Ghaffari, *Phys. Lett.* **91A**, 5 (1982).
- [49] S. W. Shaw and P. J. Holmes, *Phys. Rev. Lett.* **51**, 623 (1983).
- [50] S. W. Shaw and P. J. Holmes, *ASME J. Appl. Mech.* **50**, 849 (1983).
- [51] M. B. Hindmarsh and D. J. Jefferies, *J. Phys. A* **17**, 1791 (1984).
- [52] H. M. Isomäki, J. Von Boehm, and R. Rätty, *Phys. Lett.* **107A**, 343 (1985).
- [53] A. B. Nordmark, *J. Sound Vib.* **145**, 279 (1991).
- [54] W. Chin, E. Ott, H. E. Nusse, and C. Grebogi, *Phys. Rev. E* **50**, 4427 (1994).
- [55] C. Reid and S. Whineray, *Phys. Lett. A* **199**, 49 (1995).
- [56] J. Berg and G. A. D. Briggs, *Phys. Rev. B* **55**, 14899 (1997).
- [57] S. Salapaka, M. Dahleh, and I. Mezić, *Nonlinear Dyn.* **24**, 333 (2001).
- [58] A.-L. Barabási and H. E. Stanley, *Fractal Concepts in Surface Physics* (Cambridge University Press, Cambridge, 1995).